New Aspects in Quantitative Surface Analysis

M P Seah

Centre for Materials Measurement and Technology, National Physical Laboratory, Teddington, Middlesex TW11 0LW, UK

(Received September 28 1998; accepted December 22 1998)

The development and analysis of data bases of traceable AES and XPS reference spectra are described. The spectra have all instrumental terms calibrated and removed except the X-ray photon flux density. Auger electron intensities, in terms of the electrons emitted per steradian per incident electron for ionisation of a given shell, correlate with theory with a mean error of a factor of 1.04 with no independent fitting parameters. Correlations for $3 \leq Z \leq 83$ show that, for AES, Casnati et al's cross section for ionisation is significantly better than Gryzinski's. For inelastic mean free paths the equation TPP-2M, of Tanuma et al, is used with a cut-off for the valence electrons at 14 eV binding energy and with all 4f electrons excluded for the lanthanide metals. Correlations of experiment and theory for the data sets are now excellent. For AES a new method of using broadened differential spectra shows accuracies approaching full peak area analysis. This method has promise as a simple method for analytical use.

1. Introduction

In this study we analyse the basic formalisms for quantitative intensity measurement in AES and XPS by the use of extensive data bases of reference spectra. A data base of spectra is essential for AES since one cannot yet calculate, from first principles, the intensities of the individual peaks used for analytical work, particularly if the spectra are used in the differential mode. One can calculate, however, the total peak area intensity for Auger electrons emitted as a result of ionisation in a given shell of the atom. With a fully calibrated instrument; this peak area may be integrated, from the measured spectra, to give the number of Auger electrons emitted per unit solid angle per incident electron. This number may also be calculated from first principles to allow a comparison to be made of experiment and theory. Where such comparisons involve limited data sets a good correlation may be possible with inadequate components of the theory. Here we use data from a large data set of elements with $3 \leq Z \leq 83$, for both 5 keV and 10 keV beam energies, to ensure that fully adequate tests are possible. In this work we combine the analysis of both AES and XPS data since some aspects are best defined in the one and some in the other.

2. Experimental

The experimental data to be reported here are mainly acquired using a modified VG Scientific ESCALAB II with a 5 channel electron multiplier detector system. The system is designed for efficient AES or XPS studies. In the mode of use selected for AES the spectrometer views a uniform analytical area of 6 mm by 9 mm at the sample and so sample positioning is not at all critical. To maintain a good energy resolution the instrument is operated in the constant ΔE mode with a pass energy of 50 eV. With the 6 mm slit the spectrometer resolution is 1 eV and this is used for widescan measurements. For details of the peak regions, the slit is reduced to 1.5 mm giving an analyser resolution of 0.25 eV.

AES measurements are recorded with both 5 keV and 10 keV electron beam energies with the beam incident at 30° to the sample normal. XPS measurements are recorded with both Al and Mg X-rays with the scattering angle at 54.7°.

The intensity/energy response function of the spectrometer is measured, as described earlier [1,2], to enable the Auger electron spectra to be converted to units of electrons emitted per unit solid angle per incident electron. For XPS, the calibration is proportional to the number of electrons emitted

per unit solid angle per incident photon since there is, as yet, no simple method of accurately measuring the X-ray photon flux density at the sample.

AES measurements have been recorded for most elements of the periodic table with $3 \leq Z \leq 83$, but excluding the noble gases and radioactive elements. Most samples are analysed as elemental foils and the remainder as binary compounds. A wide range of the metallic foils have been studied in a calibrated MAC 2 analyser [3] in both the metallic and stoichiometric oxide forms. XPS measurements have been recorded for a similar range of materials.

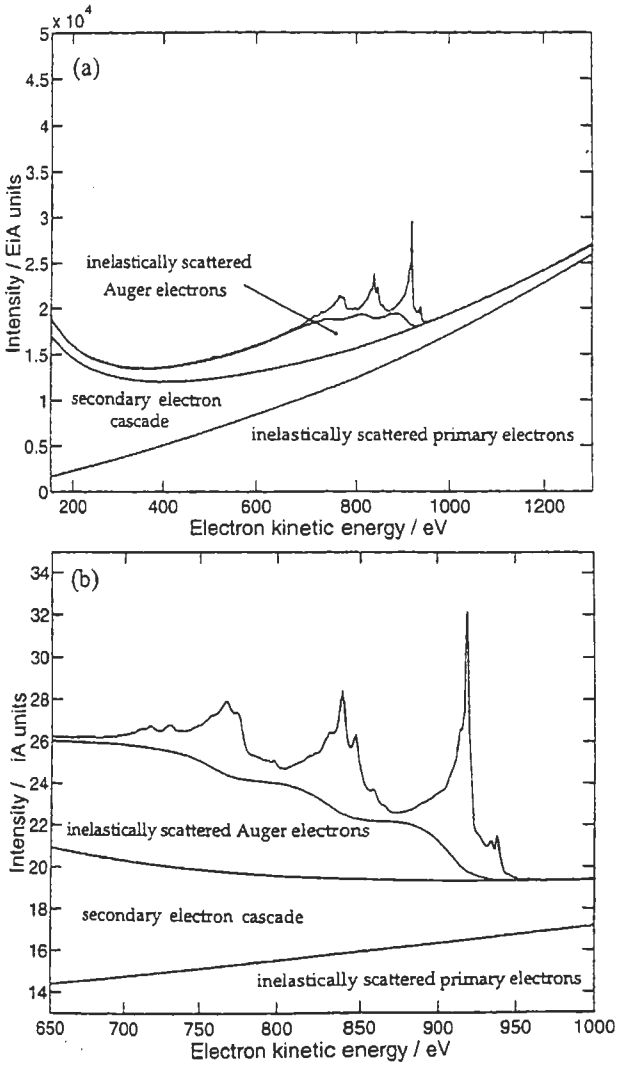

Figure 1 Copper true spectrum with the component parts of the spectrum identified: (a) survey scan in traditional $En(E)$ format, (b) detail in correct $n(E)$ format. The intensity scale is in iA units where iA is $(5.1 \pm 0.3) \times 10^{-7}$ sr^{-1} eV^{-1}.

3. Results and Discussion

In order to deduce the peak areas for Auger electron intensities from the measured spectra, the backgrounds must be removed. The backgrounds are shown in Fig 1 for the 5 keV electron beam.

First we remove the inelastically scattered primary electron background which conforms to an exponential shape [4,5]. We next remove a standard Tougaard background [6,7] using Tougaard's parameters of B and C as 3006.1 eV^2 and 1643 eV^2, respectively, deduced from the XPS data [8], and finally the secondary electron cascade [7,9]. This leaves the peak area with all background removed. Integrating this area leads directly to an intensity for, in this case, all Auger electrons with decays originating with ionisation in any of the L shells. This area is in units of electrons out per incident electron per steradian along the surface normal. Measurements for many elements are given in Fig 2 [2,8].

We may calculate these intensities in the usual way [10] but extending the calculation to sum for all of the ionisations in any given shell. The theoretical intensity for a pure element A, is given by

$$I_A^{\infty}(\text{theor},CK,E_o) =$$

$$\gamma_{AX} \sec\alpha N_A Q_A(E_{AX}) \sum_i n_{AX_i} \sigma_{AX_i}(E_o) \times [1+r_A(E^B_{AX_i},E_o,\alpha)]\lambda_A(E_{AX}) \quad (1)$$

Where γ is Burhop's factor [11], α is the angle of incidence of the electron beam, N_A is the atomic density, Q_A is Jablonski's elastic attenuation term [12], n_{AX_i} is the electron population of the level X_i ionised in the shell X, σ_{AX_i} is the ionisation cross section for an electron beam of energy E_o, r_A is the backscattering factor of Shimizu [13] and λ_A the inelastic mean free path. An analysis of many ionisation cross sections shows that the cross section of Casnati et al [14] is significantly more accurate than that of Gryzinski [15] and so only the former is used here. Gryzinski's formula may lead to errors as high as 50% [16]. For the inelastic mean free path, Tanuma et al's TPP-2M equation is

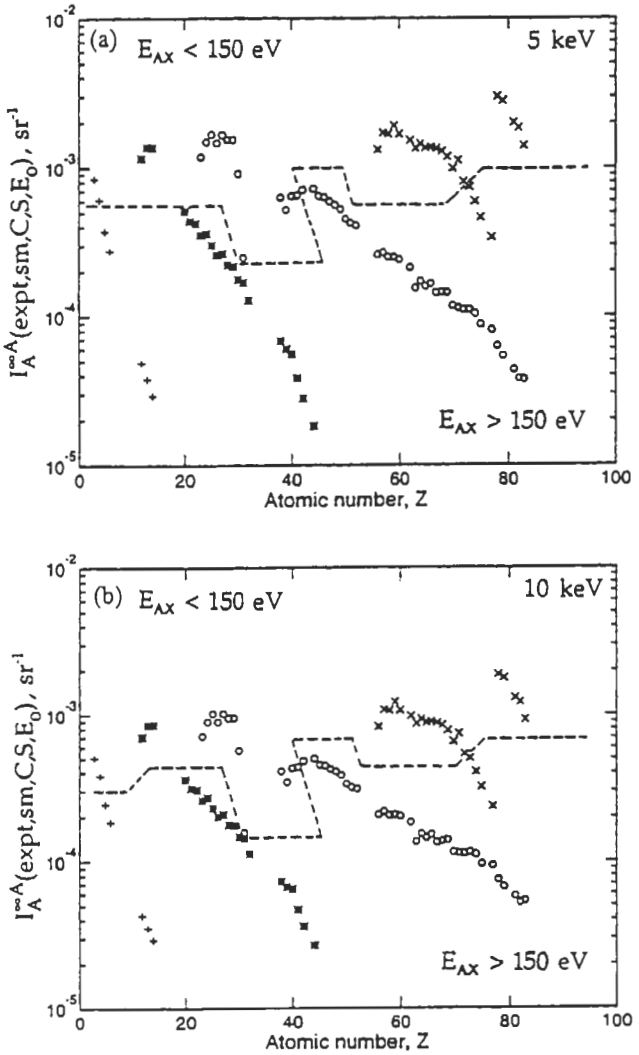

Figure 2 Experimental peak areas for the K(+), L(*), M(o) and N (x) shell ionisations at (a) 5 keV and (b) 10 keV beam energies. The points plotted above the dotted lines are for peaks below 150 eV where errors occur in the peak area measurement.

used [17]. In this equation one needs N_v, the number of valence electrons in the atom. It is not clear up to what binding energy one should include the electrons and so an analysis of the theoretical intensities, as a function of this binding energy, was made. The results [8] show that 14 eV works best. Additionally one should exclude the 4f electrons from the lanthanide metals [2,8]. The results of these calculations are shown in Fig 3.

The correlation between Figs 2 and 3 is good. Some errors are to be expected from the problem of plural emission following a single initial ionisation [8]. Care has been taken to set the area integration limits to avoid such effects. More significant is the accuracy of the Tougaard Universal function to describe all elements. On average this is good since the ratio of experiment to theory, ignoring the low energy Auger electron peaks, is 1.04. Thus, the cumulative systematic error of all of the components of the theory and the experiment is only 4%! Errors for individual elements are, of course, much larger. The greatest errors currently occur for Ca, Sc, Ti, Sr, Y, Zr. The simplicity of the experimental plots, compared with those of the theory indicate that the major error may remain with the theory.

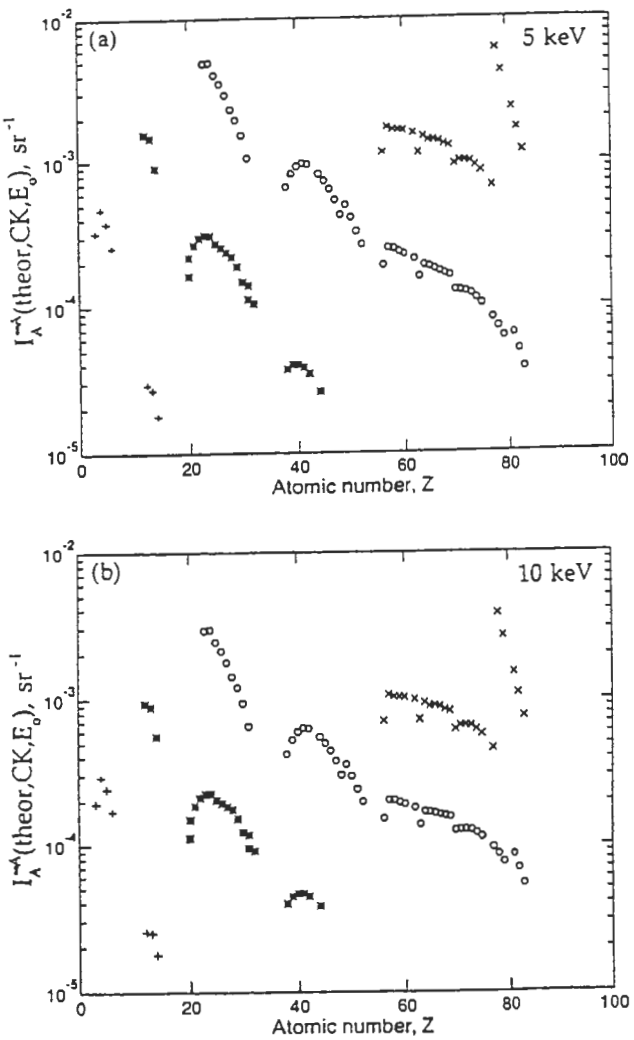

Figure 3 Calculated Auger electron intensities, excluding 4f electrons and those with binding energies above 14 eV for N_v, (a) 5 keV and (b) 10 keV.

The experiments and calculations for XPS follow closely those for AES with the ionisation cross sections taken from Scofield [18] and the anisotropy from Yeh and Lindau [19] corrected using the data of Jablonski [12]. Figure 4, shows the excellent correlation for the Mg X-ray source. By using unified data bases for AES and XPS one may separate the effects of $N_A Q_A \lambda_A$, which are common to both spectrocopies, from the other terms which are unique to the spectroscopy.

The above correlations are good for refining the theory to understand what is going on and to extrapolate and interpolate new data but, for AES, we need to consider how most analysts measure intensities. Except for alloy mixtures the peak structure in AES changes significantly on forming compounds. These shape changes make intensity measurement difficult in either the direct spectrum or the differential spectrum. An example is shown in Fig 5(a) for Mn and Mn_3O_4 [20]. These spectra have been normalised to give the same Mn peak area in the true spectrum but the 638 eV differential peak shows a factor of 1.7 difference in peak-to-peak intensity. By broadening with a 15 eV Gaussian function we see that the error is largely removed. We have broadened by a function much larger than the chemical state effects but less than one third of the major peak separations.

Analysis of the oxygen Auger electron spectra from many oxides shows that the differential peak-to-peak values for 5 eV differentials, and normalised to constant peak area, scatter over a range of a factor of 3 [20]. However, after applying a 20 eV Gaussian broadening this scatter reduces to 5% for negative peak to background measures. Thus, for practical analysis it appears that broadened differentials are nearly equivalent to the full peak area analysis but are, of course, much easier and more rapid to use.

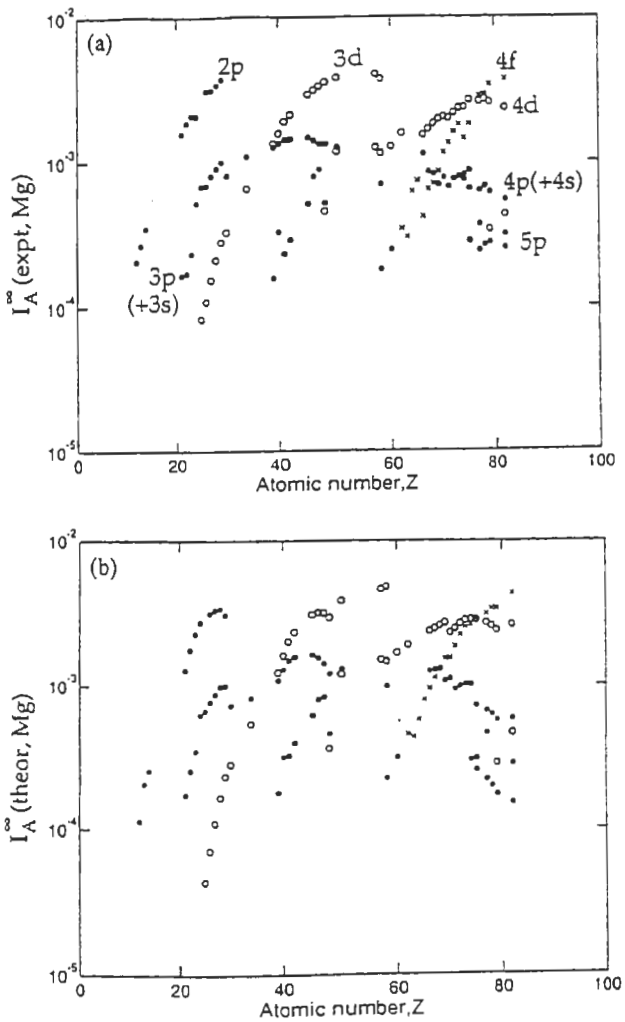

Figure 4 Measured and calculated X-ray photoelectron intensities using Mg X-rays.

4. Conclusions

By integrating traceable data bases for AES and XPS, basic aspects of the theory of quantitative surface analysis may be assessed. This allows us to test the best cross-sections to use and how to apply different aspects of the theory. It also permits a clear method to define peak areas and to obtain equivalent measures for AES. This approach shows, for instance, the popular use of Gryzinski's cross section in AES may lead to errors of up to 50%. The direct use of TPP-2M without considering the electrons to include in N_v may lead to a further error of up to a factor of 2. The direct use of differentials for measuring AES intensities may, through chemical state effects, involve a further error factor of 1.7. It is shown how these errors may be removed or reduced by the use of Casnati et al's cross section, the application of the 14 eV cut-off for N_v, the exclusion of 4f electrons and finally the use of Gaussian broadening for the measurement of differential intensities.

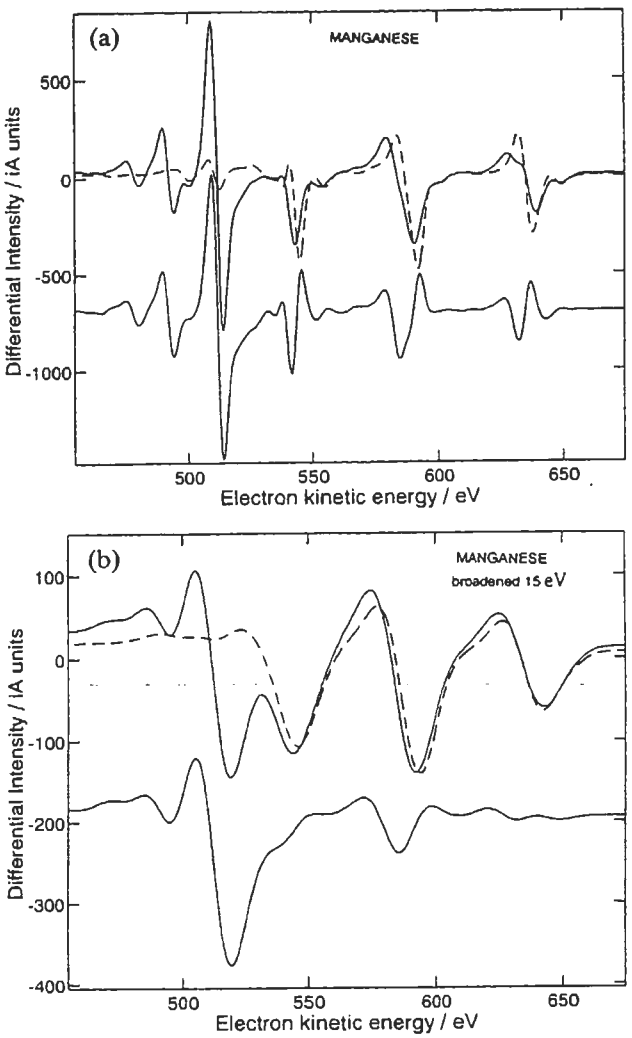

Figure 5 The differential spectra for Mn(---) and Mn_3O_4 (—) normalised to constant Mn peak area (a) 5 eV differential, (b) 15 eV Gaussian plus 5 eV differential.

5. Acknowledgements

The author would like to thank the conference organisers for inviting this review. The work in this paper was partly supported under contract with UK Department of Trade and Industry within the National Measurement System Valid Analytical Measurement Programme, and part by the Standards, Measurement and Testing Programme of the European Commission.

6. References

[1] M.P. Seah, J. Electron Spectrosc. 71, 191 (1995).
[2] M.P. Seah and I.S. Gilmore, J. Vac. Sci. Technol. A14, 1401 (1996).
[3] G. Lorang, J.P. Langeron and M.P. Seah, *ECASIA* 95, Ed H.J. Mathieu, B. Reihl and D. Briggs, p 615, Wiley, Chichester (1996).
[4] D. Jousset and J.P. Langeron, J. Vac. Sci. Technol. A5, 989 (1987).
[5] M.P. Seah and I.S. Gilmore, Surf. Interface Anal. 26, 723 (1998).
[6] S. Tougaard, Solid State Commun. 61, 547 (1987).
[7] M.P. Seah, Surf. Interface Anal. 24, 830 (1996).
[8] M.P. Seah and I.S. Gilmore, Surf. Interface Anal. 26, in the press, (1998).
[9] E.N. Sickafus, Phys. Rev. B 16, 1436 (1977).
[10] M.P. Seah in *Practical Surface Analysis Vol 1 Auger and X-ray Photoelectron Spectroscopy*, Eds D. Briggs and M.P. Seah, Chapter 5, p 201 (1990).
[11] E.H.S. Burhop, *The Auger Effect and other Radiationless Transitions*, Cambridge University Press, Cambridge (1952).
[12] A. Jablonski, Surf. Interface Anal. 23, 29 (1995).
[13] R. Shimizu, Jpn. J. Appl. Rhys. 22, 1631 (1983).
[14] E. Casnati, A. Tartari and C. Baraldi, J. Phys B 15, 155 (1982).
[15] M. Gryzinski, Phys. Rev. 138A, 336 (1965).
[16] M.P. Seah and I.S. Gilmore, Surf. Interface Anal. 26, in the press (1998).
[17] S. Tanuma, C.J. Powell and D.R. Penn, Surf. Interface Anal. 21, 165 (1994).
[18] J.H. Scofield, J. Elec Spectrosc. 8, 129 (1976).
[19] J.J. Yeh and I. Lindau, Atomic Data and Nuclear Data Tables, 32, 1 (1985).
[20] M.P. Seah, I.S. Gilmore, H.E. Bishop and G. Lorang, Surf. Interface Anal. 26, 701 (1998).